

# Current-carrying string loop motion: Limits on the classical description and shocks.

Xavier Martin<sup>a</sup> and Patrick Peter<sup>b</sup>

<sup>a</sup>*Dpto. de Física, CINVESTAV-I.P.N. A.P. 14-74-, 07000 Mexico, D.F., Mexico*

<sup>b</sup>*D.A.R.C., Observatoire de Paris-Meudon, UPR 176, CNRS, 92195 Meudon, France*

Email: xavier@fis.cinvestav.mx, Patrick.Peter@obspm.fr

(25 August 1999)

The dynamical evolution of superconducting cosmic strings is much more complicated than that of simple Goto-Nambu strings. For this reason, there are only a few known analytical solutions and no numerical ones. The goal of this paper is to present numerical solutions for the dynamics of planar superconducting cosmic string loops. In most cases, a purely dynamical approach turns out to be insufficient to describe correctly the evolution of a loop due mainly to the appearance of shocks when spacelike currents are present and kinks for timelike currents, leading to yet unaccounted for quantum effects. The consequences of the quantum effects are mostly unknown at this time because the problem requires a dynamical field theory treatment. It is however likely that ultimately the result will be massive radiation in the form of charge carriers from the string.

## I. INTRODUCTION

Cosmic strings [1] are topological defects [2] which can form in the early universe during phase transitions. The simplest kind of cosmic string is the Goto-Nambu [3] one which has no internal structure and has been studied intensively in relation with galaxy formation scenarios [4]. However, the Goto-Nambu model is by no means the only possible one. In fact, it seems likely that, if the Higgs boson triggering the cosmic string generating phase transition is coupled to charged bosons or fermions, such particles could get trapped in the strings, giving rise to conserved currents along them [5]. Such superconducting strings have non trivial internal structure (because of the existence of the current) [6–9] but were thought to be describable macroscopically by an “elastic string” formalism where the internal structure is represented by just an equation of state [10]. Even the first order corrections to dynamics due to a possible electromagnetic-type current self-interaction can be accounted for in such a way [11,12]. The dynamics of such “elastic strings” is significantly more complicated than that of Goto-Nambu strings, as can be expected, and for this reason there are very few known results on them. In particular, there is no existing example of a simulation of the dynamics of such objects, much less of a network of them. In fact, only the case where the chiral limit is taken for all strings has been treated, and then very recently [13]. In this paper will be shown the first such simulation for loops and some preliminary results derived from it.

The main known dynamical result about superconducting strings is the existence, contrary to the case of Goto-Nambu strings, of a large variety of dynamically stable loop equilibrium solutions [14,15]. This has very important consequences on the evolution of superconducting string networks since such loops at equilibrium can accumulate and become a significant part of the universe mass. In fact, these loops, called “vortons”, can

put constraints on the mass scales where superconducting strings can form, and can also be a possible solution to the dark matter problem [16,17] as well as to the ultra high energy cosmic ray enigma [18,19].

However, there are few results on the evolution of a loop toward equilibrium. A pioneering work was the study of the evolution of circular loops [20,21]. It showed that, for a significant fraction of circular initial conditions, the dynamical evolution of the loop would drive it outside of the domain of validity of the elastic string description to a domain where quantum instabilities appear and likely dominate the dynamics of the string with as yet unknown outcome [21].

In this paper, we have studied numerically the dynamical evolution of a superconducting cosmic string loop to generalize the study conducted in the circular case. First, we find that in many cases, the dynamical evolution of the loop will drive it out of the elastic regime, thereby extending the results found in the circular case. But even when the loop remains in the elastic regime, it tends to develop shocks or to fold on itself in complicated shapes, leading to a likely non-negligible chance of spontaneous charge carrier emission by quantum tunneling [24]. This suggests that the evolution of a superconducting loop toward equilibrium can not be described from a purely macroscopic point of view but must take into account purely quantum effects which result in global charge or current loss.

These new results mean that the program will have to be improved to include the treatment of shocks and string intercommutation. More importantly, it begs the question of the qualitative and quantitative consequences of the quantum effects we mentioned (which are at best very badly known), of how they can be integrated into the existing dynamical model, of the observability of the probable associated radiation, and of the consequences on the final outcome of loop evolution.

In the following section, the equations of motion for

an elastic string, of which superconducting strings are a part, are derived. In the third section, these equations are reexpressed in the way most appropriate to numerical resolution and the numerical scheme is outlined. A fourth section discusses the various equations of state (for Kaluza–Klein and superconducting strings) to be used afterwards and the stability of the various perturbation modes of a string loop endowed with such dynamics. Then, in section five, the numerical code is applied with these various equations of states on elliptic configurations as well as perturbed vorton states to exhibit the probable appearance of quantum effects through either the departure of the elastic string domain of validity, or the development of shock waves along the string, or the existence of regions of discontinuous curvature. Finally, we show that these effects should push loops toward the chiral limit and conclude in the last section.

## II. THE GENERAL EQUATIONS OF MOTION

An elastic string is described by a two dimensional worldsheet and a stress energy tensor which can be written as

$$T^{\mu\nu} = U u^\mu u^\nu - T v^\mu v^\nu, \quad (1)$$

where  $u^\mu$  is the timelike unit eigenvector of the stress energy tensor, and  $v^\mu$  is the other orthogonal, spacelike, unit eigenvector.  $U$  and  $T$  are the associated eigenvalues which can be respectively identified with the energy density and the tension of the string. In the elastic string model, they are related by an equation of state which describes the substructure of the string considered, and must be derived from a quantum field analysis [6–8]. It is useful to introduce four other thermodynamical variables,  $\mu$ ,  $\nu$ ,  $c_T^2$  and  $c_L^2$  which can be directly deduced from the knowledge of  $U$  and  $T$  by the following equations

$$\mu = \frac{dU}{d\nu}, \quad (2)$$

$$\mu\nu = U - T, \quad (3)$$

$$c_T = \sqrt{\frac{T}{U}}, \quad (4)$$

$$c_L = \sqrt{-\frac{dT}{dU}}. \quad (5)$$

$\nu$  can be interpreted as a number density variable, and  $\mu$  as an associated effective mass variable or chemical potential. We will see in the following that they are the modulus of the two conserved currents in the string. As for  $c_T$  and  $c_L$ , they can be interpreted respectively as the speeds of transverse and longitudinal perturbations along the string. They play a fundamental role in evaluating the stability of circular loops at equilibrium [14,15], and their being real (which means that the corresponding perturbations are dynamically stable) defines what we shall call the elastic regime. With the equation of state taken

into account, only one of these variables is necessary to express all six of them.

Three other tensor fields will play an important role in the following: the antisymmetric tangent tensor of the string worldsheet which can be expressed using the diad of eigenvectors as

$$\epsilon^{\mu\nu} = u^\mu v^\nu - v^\mu u^\nu, \quad (6)$$

the first fundamental tensor,  $\eta^{\mu\nu}$  which can be expressed as

$$\eta^{\mu\nu} = \epsilon^{\mu\rho} \epsilon_\rho{}^\nu = -u^\mu u^\nu + v^\mu v^\nu, \quad (7)$$

and whose mixed form  $\eta^\mu{}_\nu$  is the projector along the string worldsheet, as well as the orthogonal projector on the worldsheet

$$\perp^{\mu\nu} = g^{\mu\nu} - \eta^{\mu\nu}. \quad (8)$$

From there, the equations of motion are simply expressed as the equation of state, which can be assumed to be solved *a priori* so that only one of the thermodynamical variable is necessary to describe them all, and the conservation of the stress energy momentum tensor

$$\bar{\nabla}_\mu T^{\mu\nu} = 0, \quad (9)$$

where  $\bar{\nabla}_\mu = \eta_\mu{}^\nu \nabla_\nu$  is the covariant derivative along the string worldsheet obtained by projecting the usual derivative on the worldsheet. These equations of motion can be separated into an intrinsic part which is obtained by projection along the string worldsheet, and an extrinsic part obtained by projection perpendicularly to it [14]. Note that we do not consider here the current to be coupled with a long range interaction field such as electromagnetism. We chose this approximation (in case it would actually be coupled with such fields, which is not obvious in the first place) for three reasons: first of all, it has been shown [8,9] that as far as the internal string structure is concerned, this is utterly negligible; then for the self interaction of a loop, it was shown [12] that its leading contribution could be completely accounted for by means of a renormalization of the equation of state (like the Dirac renormalization of the classical charge of an electron). Finally, as our results show that the quantum processes are likely to be far more important than the classical radiative corrections concerning energy loss mechanisms, we have an *a posteriori* justification.

The intrinsic part of the system can be rewritten as the conservation of two currents along the string, one timelike

$$\bar{\nabla}_\rho (\nu u^\rho) = 0, \quad (10)$$

and the other spacelike

$$\bar{\nabla}_\rho (\mu v^\rho) = 0. \quad (11)$$

One of this currents corresponds to the charged current trapped in the string during the phase transition, the

other corresponds to the winding number of the string. Which is which basically depends on whether the string is in the electric sector where the charged current is time-like, or in the magnetic sector where it is spacelike. It is to be remarked for future reference that these two equations can be rewritten in adjoint form as two irrotationality equations, respectively as

$$\epsilon^{\rho\sigma}\nabla_\rho(\nu v_\sigma) = 0, \quad (12)$$

$$\epsilon^{\rho\sigma}\nabla_\rho(\mu u_\sigma) = 0, \quad (13)$$

where  $\epsilon^{\rho\sigma}$  is the antisymmetric tangent tensor defined in (6).

As for the extrinsic part of the system, it can be simplified using the explicit form of the stress energy tensor (1) as

$$\perp^\mu{}_\rho(Uu^\nu\nabla_\nu u^\rho - Tv^\nu\nabla_\nu v^\rho) = 0, \quad (14)$$

where  $\perp^\mu{}_\rho$  is the projector orthogonal to the worldsheet given by (8).

The system of equations thus includes the four equations (10), (11), (14) and the equation of state. However these equations depend explicitly only on  $u^\mu$ ,  $v^\mu$  and the four related thermodynamical parameters, and not on the string worldsheet coordinates  $x^\mu$  which are the unknowns of interest. In the following section, we will explore the various ways to connect these equations to the worldsheet coordinates through gauge fixing conditions and find the best way to simulate the dynamics of a cosmic string loop.

### III. THE SIMULATION

One possibility to solve the dynamical equations would be to choose  $u^\mu$  and  $v^\mu$  as unknowns and integrate the worldsheet back from them, a process which however introduces two extra unknowns. The corresponding two extra equations come from an integrability condition [14]

$$K_{[\mu\nu]}{}^\rho = 0, \text{ where } K_{\mu\nu}{}^\rho = \eta^\sigma{}_\mu \overline{\nabla}_\nu \eta^\rho{}_\sigma \quad (15)$$

is the second fundamental tensor of the string.

Thus, it seems much better to choose the string worldsheet coordinates  $x^\mu(\tau, \sigma)$  as unknown. The timelike internal parameter of the worldsheet  $\tau$  should be identified with the time coordinate to ensure an easy representation of the evolution of the solution in time. The other internal parameter  $\sigma$  must be chosen so that the expression of  $u^\mu$  and  $v^\mu$  as functions of the worldsheet coordinates be straightforward. The simplest choice is to choose the potential associated with the irrotationality equation (12) which we will denote  $\psi$ . The meaning of this potential will depend of the sector, electric or magnetic, considered. In the magnetic sector,  $\psi$  can be interpreted as the phase of the charge carrier field, whereas in the electric sector it is a dual potential whose gradient is orthogonal

to that of the phase of the charge carrier. This ensures  $\psi$  to be a spacelike coordinate whatever the sector considered. Then, there only remains three unknowns  $\mathbf{x}(t, \psi)$  and three equations (11) and (14) since the fourth (10), which is equivalent to (12), is automatically solved by the choice of  $\psi$  as internal parameter of the worldsheet.

With this choice of unknowns, the other variables which appear in the equations of motion are expressed as

$$u^\rho = \frac{\dot{x}^\rho}{\dot{z}}, \quad (16)$$

$$v^\rho = \frac{1}{n\dot{z}}(\beta\dot{x}^\rho + \dot{z}^2 x'^\rho), \quad (17)$$

$$\nu = \frac{\dot{z}}{n}, \quad (18)$$

where dots and primes denote respectively derivative with respect to  $t$  and  $\psi$ , and where several new notations have been used to contract these expressions:

$$\dot{z} = \sqrt{-\dot{x}^\rho \dot{x}_\rho}, \quad (19)$$

$$z' = \sqrt{x'^\rho x'_\rho}, \quad (20)$$

$$\beta = x'^\rho \dot{x}_\rho, \quad (21)$$

$$n = \sqrt{\beta^2 + z'^2 \dot{z}^2}. \quad (22)$$

Note also that the equation of state and the two equations (2)-(3) enable to express the three other thermodynamical parameters  $U$ ,  $T$  and  $\mu$  as functions of  $\nu$  only and thus of  $\mathbf{x}(t, \psi)$ . Replacing all these expressions in equation (11) gives

$$\mathbf{v} \cdot [(n^2 - \beta^2 c_L^2)\ddot{\mathbf{x}} - \dot{z}^4 c_L^2 \mathbf{x}'' - 2\beta\dot{z}^2 c_L^2 \dot{\mathbf{x}}'] = 0, \quad (23)$$

where  $\mathbf{v}$  is just the spatial part of  $v^\rho$  as defined in (17).

As for the extrinsic equation (14), it becomes:

$$\mathbf{w}_{1,2} \cdot [(n^2 - \beta^2 c_T^2)\ddot{\mathbf{x}} - \dot{z}^4 c_T^2 \mathbf{x}'' - 2\beta\dot{z}^2 c_T^2 \dot{\mathbf{x}}'] = 0, \quad (24)$$

where  $\mathbf{w}_{1,2}$  are the spatial part of two independent quadrivectors orthogonal to the worldsheet. Two such vectors can always be chosen among the three following vectors:

$$w_{\perp 1}^\rho = (\dot{x}_1 x'_2 - \dot{x}_2 x'_1, x'_2, -x'_1, 0), \quad (25)$$

$$w_{\perp 2}^\rho = (\dot{x}_1 x'_3 - \dot{x}_3 x'_1, x'_3, 0, -x'_1), \quad (26)$$

$$w_{\perp 3}^\rho = (\dot{x}_3 x'_2 - \dot{x}_2 x'_3, 0, -x'_3, x'_2). \quad (27)$$

Finally, the equation of state is assumed to be solved *a priori* to get  $c_T^2$  and  $c_L^2$  as functions of  $\nu$  which is itself a function of the unknowns through (18).

The actual system we now have to solve can be conveniently re-expressed in a simpler way by restricting its motion to be in a plane,  $x_3 = 0$  for instance. Then, only the vector  $w_{\perp 1}^\rho$  gives a non trivial equation in (24). The set of dynamical equations is now given by the two equations (23) and (24) which can be solved to find that the functions  $x(t, \psi)$  and  $y(t, \psi)$  satisfy

$$\ddot{x} = \frac{1}{n^2}[Ax' + B(y' - \Delta\dot{x})], \quad (28)$$

$$\ddot{y} = \frac{1}{n^2}[Ay' - B(x' + \Delta\dot{y})], \quad (29)$$

where the functions  $A$  and  $B$  are given by

$$A = \frac{\dot{z}^2 c_L^2}{n^2 - \beta^2 c_L^2} [\dot{z}^2 (c_1 x'' + c_2 y'') + 2\beta(c_1 \dot{x}' + c_2 \dot{y}')], \quad (30)$$

$$B = \frac{\dot{z}^2 c_T^2}{n^2 - \beta^2 c_T^2} [\dot{z}^2 (x'' y' - x' y'') + 2\beta(\dot{x}' y' - x' \dot{y}')], \quad (31)$$

with

$$c_1 \equiv x' + \Delta\dot{y}, \quad c_2 \equiv y' - \Delta\dot{x}, \quad \Delta \equiv \dot{x}y' - \dot{y}x'. \quad (32)$$

Obviously the dependence of the worldsheet position  $\mathbf{x}(t, \psi)$  in  $\psi$  must be periodic for a loop, with a constant period  $L$  given by the conserved quantity associated with the conserved current (10)

$$L = \oint (\nu u^0) \sqrt{-\eta} d\psi = \oint d\psi. \quad (33)$$

The string worldsheet can then be discretized on a grid with  $N$  spatial points, and a variable time-step  $\delta$ . Since the equations of motion are of second order, the worldsheet is then described at a given time-step by  $2N$  vectors

$$\mathbf{x}_{ij} \simeq \mathbf{x}(i\delta, \frac{j}{N}L), \quad (34)$$

$$\dot{\mathbf{x}}_{ij} \simeq \dot{\mathbf{x}}(i\delta, \frac{j}{N}L), \quad (35)$$

and the equations of motion (28)-(29), discretized through a finite difference scheme, then enable to calculate the  $2N$  vectors at the next time-step  $i + 1$ . The time-step is automatically adjusted by the program so that the finite difference scheme remain stable. The total energy

$$E_T \equiv \oint d\psi \frac{U[\nu(\psi)]}{n\dot{z}^2} (n^2 - \beta^2 c_T^2) \quad (36)$$

and angular momentum

$$J_T \equiv \oint d\psi \frac{\beta U n}{\dot{z}^2} (1 - c_T^2) \quad (37)$$

of the system, which are obviously conserved by the equations of motion, serve as controls of the deviations of the numerical approximation from the exact solution. In the following, the relative errors on the energy and angular momentum are always kept to less than  $10^{-6}$  over all the time evolution followed, unless specified otherwise (as will be the case for instance due to the appearance of uncontrollable quantum effects).

#### IV. EQUATION OF STATE

The equation of state is what differentiates the various elastic string models. From a single elastic string model, there will generally arise two different equations of state depending on whether the current condensed inside the string is timelike or spacelike. These two regimes of the model will be called respectively electric and magnetic. In practice, there exists two elastic string models of physical interest: the transsonic model (also called wiggly Goto–Nambu model or Kaluza–Klein model), and the superconducting model.

The transsonic string is a simple model which can arise in various ways. It is for instance the effective model to represent a wiggly Goto–Nambu string [22,23], but it can also be found to arise from the compactification of strings in a 5-dimensional Kaluza–Klein theory. One of the peculiarities of the wiggly Goto–Nambu model is that it is self-dual, meaning that the equations of state in the two regimes are the same, given by

$$UT = m^4, \quad (38)$$

with  $m$  a constant having the dimension of a mass. Here and in what follows, the mass  $m$  is essentially the characteristic symmetry breaking scale at which the strings form. In the case of a wiggly Goto–Nambu string, it is also the value of the equal energy density and tension of the bare Goto–Nambu string.

It is then possible to derive the variable  $\nu$  from (2) and (3) as

$$\nu = m\sqrt{U^2 - m^2}, \quad (39)$$

and from there the expressions of the two speeds of perturbations as functions of  $\nu$  as required by the equations of motion (28) and (29):

$$c_T^2 = c_L^2 = (1 + \nu_*^2)^{-1}, \quad (40)$$

where  $\nu_* = \nu/m$  is a dimensionless variable.

The fact that the two speeds of transverse and longitudinal perturbations are equal is a characteristic of this model, and the reason it is sometimes called the transsonic model. Another consequence of the equality of these two speeds is that this model can be exactly solved in flat space [23], as could be expected from the fact that it is the effective model of a Goto–Nambu string, model which shares this same property. The simplicity of this model makes it ideal to test the simulation code before going on to the more difficult superconducting string models.

The other physically interesting type of elastic string equations of state arise when studying superconducting strings. Actual realistic models for string superconductivity coming from field theoretical models in four dimensions require two different mass scales, namely the string scale  $m$ , already introduced, which is also the string forming symmetry breaking scale, and the mass  $m_*$  which is

the one at which the current sets up, i.e. it is roughly the mass of the current carrier. Also such models have been found to be definitely not self dual, and one therefore needs to know the equations of state in the two separated electric and magnetic regimes. In this paper, we adopt the most reasonable model of superconducting cosmic string existing to date [25].

### A. The magnetic regime

In the magnetic regime, it can be seen that the equation of state derived in [25] gives

$$c_T^2 = \frac{1}{1 + \nu_*^2} \frac{2m^2(1 + \nu_*^2)^2 - \nu^2(1 - \nu_*^2)}{2m^2(1 + \nu_*^2) + \nu^2}, \quad (41)$$

$$c_L^2 = \frac{1 - 3\nu_*^2}{1 + \nu_*^2}, \quad (42)$$

where now  $\nu_* = \nu/m_*$ . Here,  $\nu_*^2 < 1/3$  to insure that  $c_L^2$  remains everywhere positive. It is dynamically possible for  $\nu$  to go above this value (as will be seen below), but then the string becomes unstable with respect to longitudinal perturbations and the elastic string description we adopted to describe the dynamics of the string breaks down due to quantum instabilities in the string. As we will see below, most of the string loop trajectories, independently of the initial conditions, develop shock waves, the description of which is beyond the scope of the simulation presented here.

### B. The electric regime

In the electric regime, the best fit to the equation of state which also satisfies the phase frequency threshold behavior [7,30] was also derived in [25] and gives for our purpose

$$c_T^2 = 1 - \frac{2X_*}{[2m^2/m_*^2 + \ln(1 - X_*)](1 - X_*) + 2X_*}, \quad (43)$$

$$c_L^2 = \frac{1 - X_*}{1 + X_*} \quad (44)$$

$$X_* = \frac{2\nu_*^2 + 1 - \sqrt{4\nu_*^2 + 1}}{2\nu_*^2}, \quad (45)$$

where, as previously,  $\nu_* = \nu/m_*$ , and  $\nu$  is bounded  $\nu < \sqrt{e^{2m^2/m_*^2} - 1}$ , but this time so that  $c_T^2 > 0$ . Again, it is dynamically possible for  $\nu$  to go above this value (as will be seen below), but then the string becomes unstable with respect to transverse perturbations and the elastic string description we adopted to describe the dynamics of the string breaks down due to quantum instabilities in the string. In this regime, near the critical current (which can become large with respect to  $m$  contrary to the magnetic regime), if the current in the string can interact electromagnetically, the dynamical corrections due

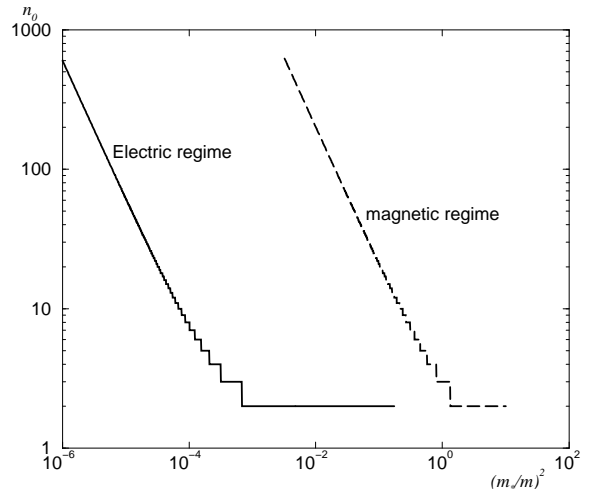


FIG. 1. First unstable equatorial mode number found when the current grows up from 0, for the electric (full line) and magnetic (dashed line) regimes, as a function of the square mass ratio  $(m_*/m)^2$ .

to the current self-interaction become large and an effective equation of state must be used to take them into account to first order [12,21]. This effective equation of state is not expected to change significantly the qualitative results of this paper and will therefore be ignored in the following.

### C. Stability

Circular rotating configurations are known to be equilibrium states, often called vortons, with stability depending on the perturbation mode number and the two perturbation velocities  $c_L$  and  $c_T$ . In other words, whether a mode is stable or not essentially depends on the relevant equation of state. Note that, although only equatorial perturbations (i.e. in the plane of the loop) are considered here, transverse perturbations (i.e. orthogonal to the plane of the loop) are always stable and would not therefore introduce any new special behavior. For the Kaluza-Klein self-dual model discussed above, stability is ensured whatever the mode number since in this case  $c_L = c_T$ . This fact will enable us to describe any perturbed equilibrium loop configuration without difficulty, the loop being unable to leave the region where the elastic description is valid. However, this is no longer the case for realistic superconducting string models, such as the one described above, since the squared velocities  $c_L^2$  and  $c_T^2$  can now become negative, in which case the macroscopic description becomes insufficient and microscopic (quantum) effects should therefore be taken into account. Moreover, the perturbation velocities are no longer always equal, and one must use the full stability formalism [15] to derive the complicated relation between

the mode numbers  $n$ , corresponding to perturbations of the type

$$r = R_0 + \delta R \exp[i(\omega t - n\theta)], \quad (46)$$

with  $(r, \theta)$  the polar coordinates in the loop plane and  $\omega$  the angular velocity of the mode, and their stability. As both these models basically depend on a single parameter, namely the mass ratio  $m_*/m$ , we present here the regions for which instability is likely to occur as a function of the mass ratio.

Fig. 1 shows the first unstable mode number found when the current grows from 0, for each model, as a function of the mass ratio  $(m_*/m)^2$ . The curve in the electric regime stops at  $m_*^2/m^2 \simeq 0.65$  because beyond this point all vortons are stable [26], and the first unstable mode therefore does not exist. It can also be argued that for moderately small ratio  $m_* \lesssim 10^{-3}m$ , the first unstable modes are found for  $n \sim 10^3$ , and these modes require large amounts of energy to be excited. This means that if, as proposed by many realistic superconducting string models, the current carrier is reasonably less massive than the string forming Higgs field, then the vortons formed are likely to be almost stable, even from a cosmological point of view. We have therefore used the results of Figs. 1 to investigate only those low  $n$  (in practice less than ten) that are easily excited and unstable. This means we have concentrated our attention in what follows on square mass ratios ranging from a  $10^{-4}$  to unity. This does not mean that this parameter should be found in such a range but simply that this is the region of parameter space where interesting effects are supposed to take place.

A final conclusion that can be drawn from Fig. 1 is that the instability regions are widely separated between spacelike and timelike currents. This mean in practice that given the effective value of the mass ratio, the evolution of the spacelike and timelike distribution could be qualitatively very different, as for  $m_*/m \lesssim 10^{-2}$ , the magnetic vortons are almost stable, with first unstable mode greater than a thousand, while the electric vortons suffer instabilities already for the  $n = 2$  mode, although it should be remarked that those vortons carrying very strong timelike currents are expected to be completely stable [26,27]

## V. EVOLUTION

The code was first tested on some of the few known exact solutions. For instance, equilibrium states are left stationary for as long as we care to run the program. Similarly, stable circular modes are found stable by the program while unstable ones do start leaving equilibrium almost immediately. The program is not capable to determine with certainty what is the long range evolution of these unstable modes due to the fact, discussed below, that other effects should be taken into account in their

description. Another clue that the program is performing well is that it conserves circularity for as long as we care to run it and reproduces exactly the results of Ref. [21].

Since circular solutions have been analyzed analytically in detail [21], we show in this chapter the numerical evolution of elliptic initial configurations and of various perturbed vorton states, stable and unstable.

First was investigated the fate of elliptic loops and equatorial perturbations of vortons (46) with the transsonic equation of state, as it is simpler and yields only stable vorton modes. Elliptic configurations present the advantage of showing all the non-linear effects right from the beginning of the simulation, whereas the stable equatorial modes enable to check the program and give a reference before studying unstable modes with the superconducting equations of state.

Then the more complicated superconducting equations of state presented in chapter IV are investigated, again using elliptic configurations and equatorial perturbations of vortons. For elliptic initial configurations, in both regimes (magnetic or electric), examples of time evolution similar to that of the transsonic string were obtained, and are not shown again. However, in some instances, completely different (and in some cases unexpected) dynamics were found, leading to drastic modifications in our understanding of the dynamics of a cosmic string loop. As for perturbed vortons, since stable ones obviously yield the same results as in the transsonic case, only unstable perturbation modes are shown. The latter start evolving in the linear approximation, but because they are unstable must grow exponentially, becoming more and more non-linear as time passes. A systematic study was done to find the generic behavior of these unstable modes.

### A. Kaluza–Klein strings

The first series of simulations performed concern elliptic loops, for which the initial configuration reads

$$x(t = 0, \psi) = R \cos\left(\frac{\psi}{R\gamma\nu_0}\right), \quad (47)$$

$$\dot{x}(t = 0, \psi) = -\frac{c_T}{1 + \varepsilon} \sin\left(\frac{\psi}{R\gamma\nu_0}\right), \quad (48)$$

$$y(t = 0, \psi) = R e \sin\left(\frac{\psi}{R\gamma\nu_0}\right), \quad (49)$$

$$\dot{y}(t = 0, \psi) = \frac{c_T}{1 + \varepsilon} \cos\left(\frac{\psi}{R\gamma\nu_0}\right), \quad (50)$$

where  $\nu_0$  is the initial value of the state parameter, assumed constant along the worldsheet,  $e$  is the ellipticity of the configuration (for  $e = 1$ , one gets a circle of radius  $R$ ), the spacelike coordinate  $\psi$  varies from zero to

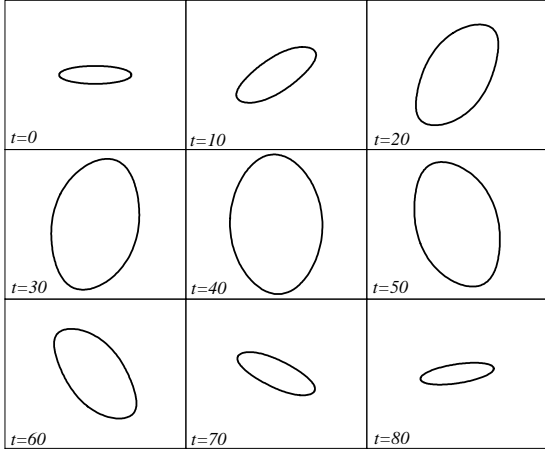


FIG. 2. Elliptic configuration evolution for a Kaluza–Klein equation of state. Here,  $e = 0.3$  and  $\nu_{*0}^2 = 1$ . The periodic evolution reveals that the loop size increases while its shape is conserved.

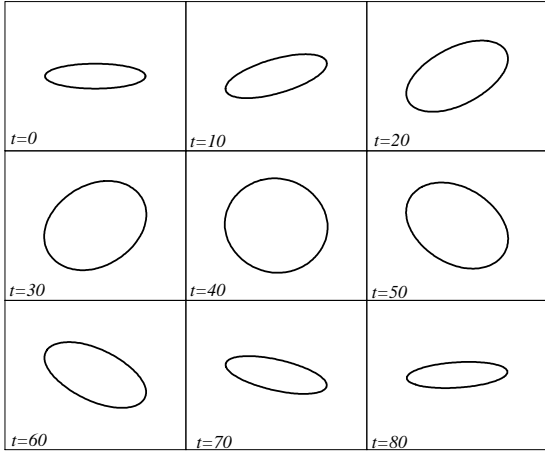


FIG. 3. Same as Fig. 2 with now  $\nu_{*0}^2 = 0.1$ . In this particular case, the shape also changes, becoming almost circular at about half the period.

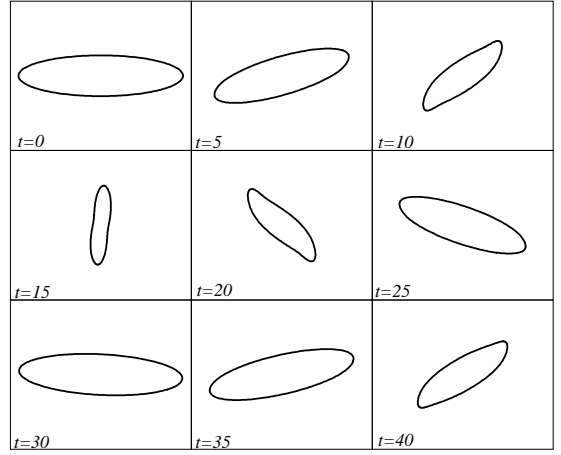


FIG. 4. Same elliptic configuration evolution as on Fig. 2 but with the velocity parameter set to  $\varepsilon = 0.1$ . It is seen that the shape is modified drastically even though the departure from equilibrium is relatively modest.

$2\pi R\gamma\nu_0$ , and  $\gamma = (1 - \dot{x}^2 - \dot{y}^2)^{-1/2}$  is the (constant) initial Lorentz factor; the dimensionless parameter  $\varepsilon$  measures the deviation in velocities from the equilibrium state obtained when  $e = 1$  and  $\varepsilon = 0$ .

The first two figures, namely Figs. 2 and 3, show two different kinds of such equilibrium configurations for which  $\varepsilon = 0$ . These figures differ only in their initial state parameter  $\nu_0$  and are presented to show that the ellipticity can be, either conserved as in Fig. 2, or made to vary greatly as in Fig. 3 where the loop becomes almost circular halfway through its periodic evolution.

Getting further away from equilibrium is very simply achieved by increasing the value of the parameter  $\varepsilon$ . On Fig. 4 is shown the evolution of a loop with the same initial conditions as on Fig. 2 but with  $\varepsilon = 0.1$ . During the loop evolution now, as the initial velocity has been slightly reduced, the loop size decreases, which was expected. Shapes similar to those of Figs. 2 and 3 are produced, with a loop size increasing, for negative values of  $\varepsilon$ . What is more interesting however is the shape of the loop which is very strongly deformed during its quasi-periodic motion. As is seen on Fig. 4, regions of relatively large curvature tend to be formed. These points are good candidates for charge carrier emission.

Exaggerating even more the value of  $\varepsilon$  yields Fig. 5, where cusps are now formed, i.e. points where the curvature diverges, and the string loop shows points where intercommutation should be occurring. The treatment of the ensuing evolution is beyond the scope of the elastic string description and therefore, even though the simulation goes on very well at these points, we believe the relevant physics not to be taken into account properly from this time on. For instance, charge carriers will also be emitted at such points. In the case of the wiggly Goto–

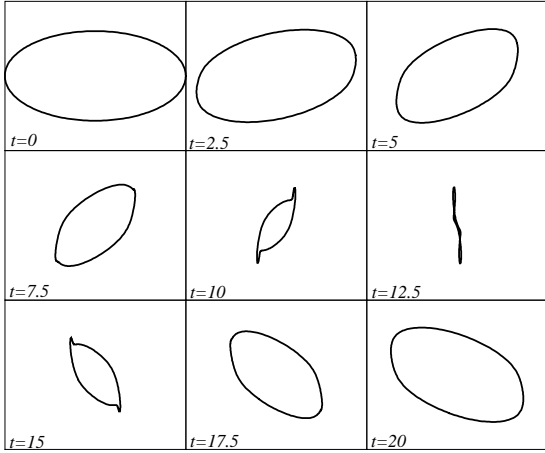


FIG. 5. Same as Fig. 4 but with a larger velocity deviation  $\varepsilon = 1$ . The loop contracts so much as to attain infinite curvature, i.e. points where intercommutation should be taking place.

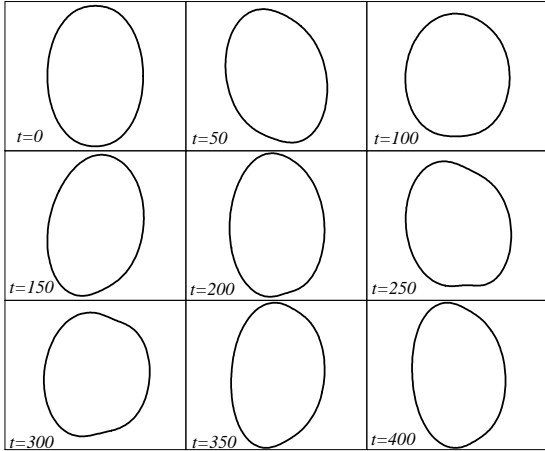


FIG. 6.  $n = 2$  perturbation mode of a transsonic vorton with a rather high amplitude of  $\delta R/R = 0.6$ .

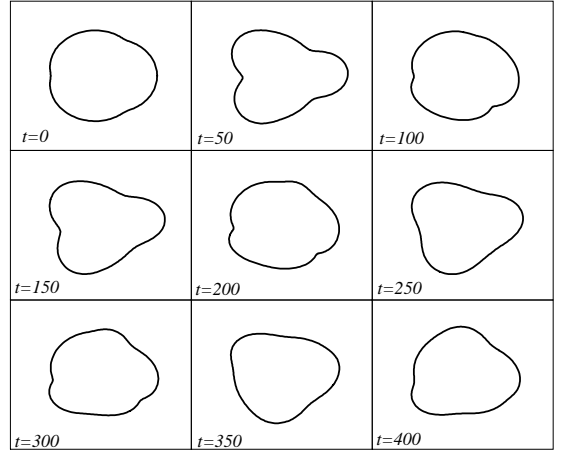


FIG. 7. Same as Fig. 6 for the mode  $n = 3$ .

Nambu string model, this emission will take the form of microscopic loops produced by intercommutation of the microstructure moving in the string. As will be discussed further down, this emission should be evaluated as it is a fairly generic situation in this model but also in the superconducting string one.

Let us now turn to the fate of circular “vorton” states with equatorial perturbations of the form (46). Figs. 6, 7 and 8 show the evolution for the modes  $n = 2, 3$  and 4. Since we have seen that transsonic vortons are always stable, a high perturbation value for  $\delta R/R \simeq 0.5$  could be used. Here again, it is found that the motion is quasi-periodic and that the shape is very strongly modified during a period. It is interesting to note however that even though the evolution we investigated involved non linear effects because of the large amplitude used, the modes remain almost completely decoupled throughout the loop trajectory. This is to be contrasted to what happens with the other equation of state corresponding to actual particle condensates in strings and to which we now turn.

## B. The magnetic shock

Let us start with an unstable mode  $n = 3$  as exemplified on Fig. 9. On this figure is plotted not the actual string loop trajectory, as nothing visible to the naked eye could then be seen: even the amplitude of the perturbation does not have time enough to increase before the important effect takes place, and what is seen is just the ordinary rotation of the unperturbed loop. Instead, what we show is the gauge invariant and rescaled state parameter  $\nu_\star^2$  as a function of the spacelike string internal coordinate  $\psi$ , in our case the point label. Although this coordinate is, by its very definition, not gauge invari-



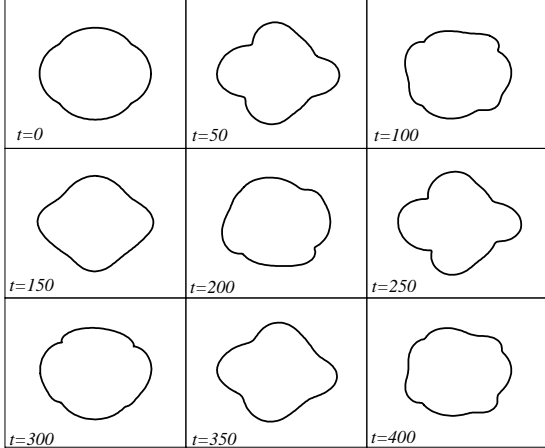


FIG. 8. Same as Fig. 6 for the mode  $n = 4$  and  $\delta R/R$  lowered to 0.45.

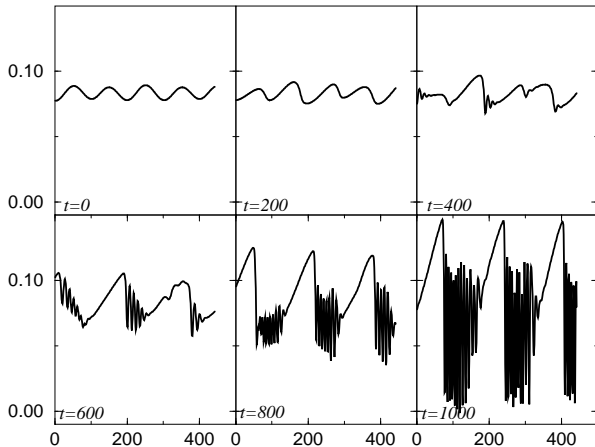


FIG. 9. Time evolution of the state parameter  $\nu_*^2$  along the string worldsheet for an unstable mode  $n = 3$  in the magnetic regime. This figure is for the magnetic equation of state with mass ratio  $m_*/m = 1$  and initial mean state parameter  $\nu_* = 0.3$ . It shows the development of a physical shock as it is clear that  $\nu$  is indeed a gauge invariant quantity. When the discontinuity becomes too important to handle for the program, the Gibbs phenomenon occurs, as expected, and the simulation ends.

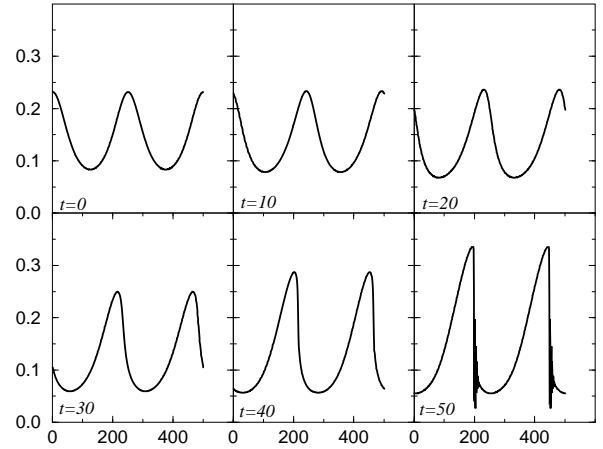


FIG. 10. Same as Fig. 9, but for an elliptic initial configuration with  $e = 0.6$ . Again, shocks develop, and in much the same way as if it was an unstable  $n = 2$  initial configuration.

ant, the same results apply when  $\nu_*$  is plotted again say, the  $x$  position coordinate of the loop, with the advantage of showing an unwrapped picture. This simulation used 500 space points and clearly shows that a shock wave is being formed at three different points (whose precise position is physically irrelevant but that are located at equal distances from each other, thereby preserving the original symmetry) along the string worldsheet. This is a generic conclusion for unstable modes: a mode of index  $n$  will develop, in the magnetic regime,  $n$  shock fronts. As can be seen from the figure, when the discontinuity forms, small oscillations appear which are not physical but instead reflect the occurrence of the well-known Gibbs phenomenon, produced by the simulation scheme which cannot, with a uniform grid, describe shocks. This figure also shows that the shocks tend to increase the amplitude of variation of the current.

Fig. 10 shows a similar evolution pattern for an initially elliptic configuration. In this particular case, it is clear from the periodicity that the leading mode would be  $n = 2$ , even though all the unstable modes are actually present in this initial configuration. This is translated in the figure by the presence of only two shock fronts. In this figure, and contrary to the previous case, the shock can actually drive the configuration outside the range of validity of the elastic string description, as  $\nu_*^2$  can reach values greater than a third for which the longitudinal perturbation velocity ceases to be real. Two possibilities are thus opened: either the shock occurs while the string is still in the elastic regime, or the longitudinal dynamical instability occurs before the shock is completed. In both situations however, we believe our simulation to stop giving an accurate description of the phenomena that should be taking place.

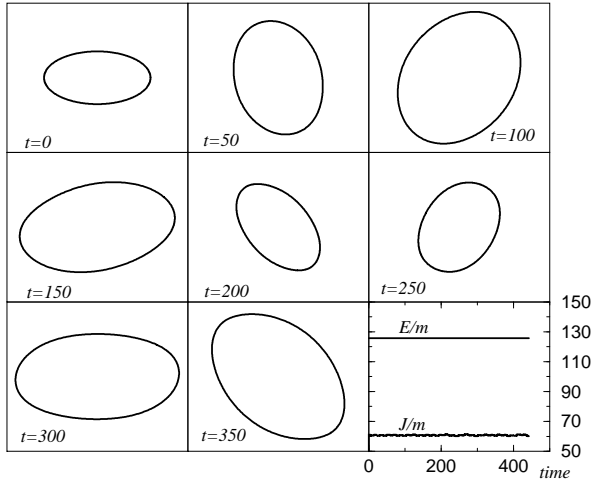


FIG. 11. Time evolution of essentially the same elliptic configuration as on Fig. 10 but in the electric regime instead. In this regime, no shock can develop, as shown in Fig. 12. The bottom-right corner shows the total energy and angular momentum of the loop versus time, and they are almost exactly conserved during the quasi-periodic evolution.

To continue further the simulation would require a semi-classical treatment of the quantum effects that are expected to take place where the shocks form. Most probably, the leading effect will be to emit one current-carrier particle anywhere the state parameter becomes discontinuous. This fact entitles us to cast serious doubts as to the actual formation of shocks in cosmic string loops: contrary to its analog in fluid dynamics, a string shock lives in two dimensions, the string worldsheet, that is embedded in the four dimensional space time, thus opening the phase space to particle emission. As a result, the energy contained in the shocks can be released in such a way as to smooth it out. From subsection VD, such an effect would lead to current loss, so that the loop distribution must favor the chiral limit in network simulations. More detailed studies must however be carried on before any definite conclusion can be reached on that point.

### C. The electric kink

To see what happens in the electric regime and check the result of Ref. [28] according to which no shock should take place, we have performed a simulation with exactly the same initial parameters as Fig. 10, but now for a timelike current and the equation of state of the electric regime. Fig. 11 shows the spatial configuration of the loop, with an evolution very similar to that of the transsonic string loop, while Fig. 12 shows the evolution of the state parameter. This completely stable and quasi periodic motion develops an harmonic frequency which is subsequently smeared out. This effect, which prevents

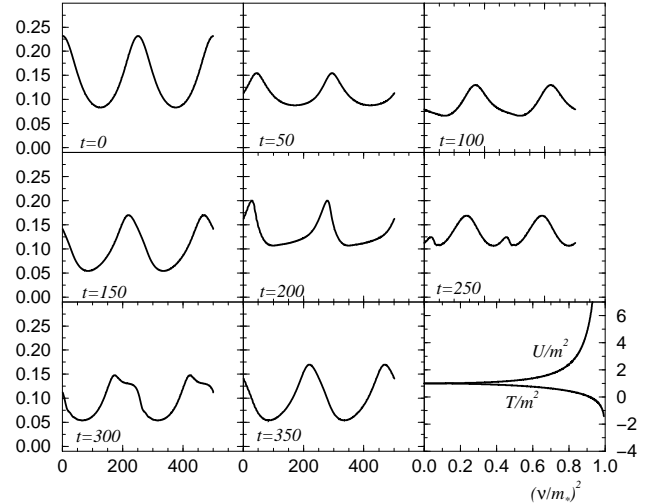


FIG. 12. Time evolution of the state parameter  $\nu_*^2$  against the point labeling function  $\psi$  for Fig. 11. Contrary to what happened in the magnetic case, the harmonic developed by the state parameter is smoothed out. The bottom-right corner recalls the equation of state  $U/m^2$  and  $T/m^2$  as functions of  $\nu_*^2$ .

the apparition of shocks, was found to occur any time a shock was expected to form in the electric regime. As a result, we claim that, indeed, no shock can be formed in a timelike current carrying cosmic string loop, at least through ordinary dynamical effects.

Instead of shocks, electric string loop evolution exhibits an unexpected feature, namely the appearance of what is usually called kinks. These are regions, shown for instance on Figs. 13 and 15, where the curvature of the string becomes discontinuous, and the state parameter tends to unity (Figs. 14 and 16), limit where, as recalled on these latter figures, the tension reaches negative values. Thus, at these points the string leaves the domain of validity of our dynamical formalism likely resulting, again, in particle emission and as shown in subsection VD, evolution of the end vorton toward the chiral limit and thus better stability.

An astonishing point is the number of kinks formed: we have found generically that an unstable equatorial mode of index  $n$  yields exactly  $2n - 1$  kinks. We could not find any explanation for this completely general result.

Therefore, it appears to be unavoidable that, in both domains, cosmic string loops will radiate charge carriers. The exact processes whereby it can do so has to be explored in more details and in particular quantified. As long as this has not been done, the consequences on the evolution and decay of superconducting cosmic string loops will remain sketchy at best.

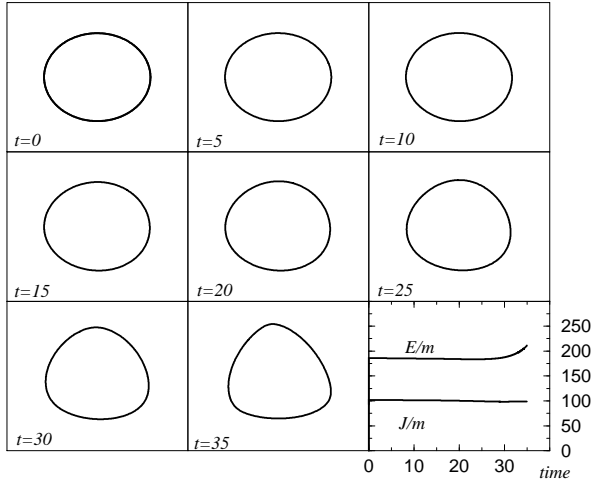


FIG. 13. Time evolution of the  $n = 2$  unstable mode for an electric loop with mass ratio  $(m_*/m)^2 = 0.1$  and initial value of the state parameter  $\nu_{*0}^2 = 0.3$ . The loop shape is modified until three kinks, i.e. regions of discontinuous curvature, are formed and the total energy is no longer conserved, meaning the elastic string description is insufficient.

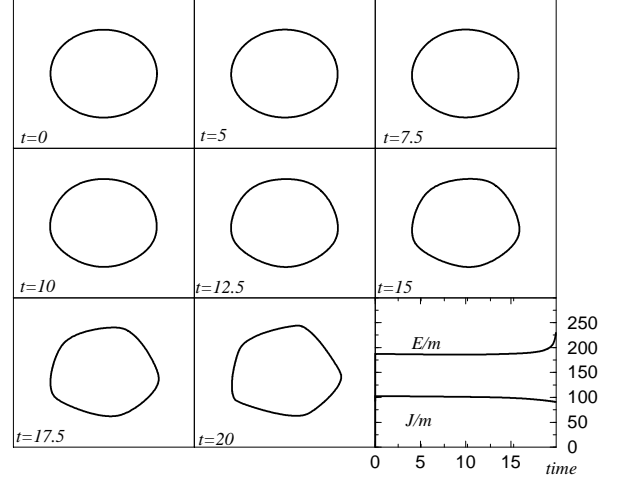


FIG. 15. Same as Fig. 13 for a mode  $n = 3$ . In this case, one finds that five kinks develop.

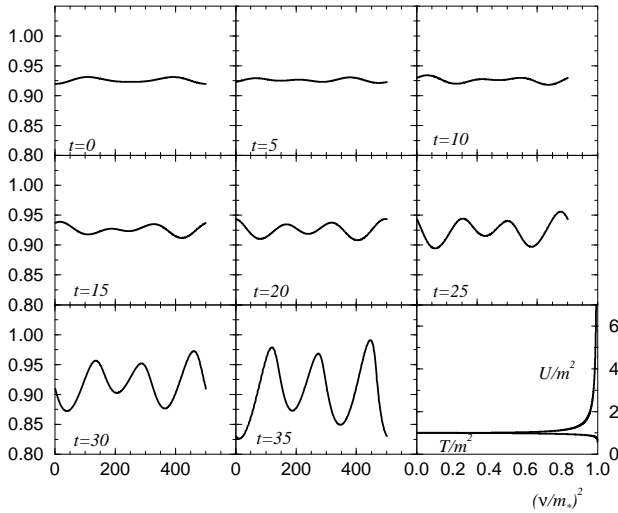


FIG. 14. Same as Fig. 13 for the state parameter versus the point labeling. As  $\nu_*$  goes to large values, approaching unity, the dynamics drive the tension to negative values.

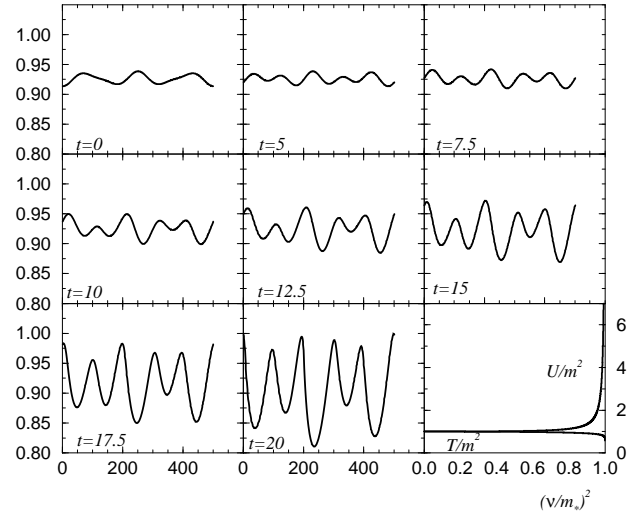


FIG. 16. Same as Fig. 15 for the state parameter versus the point labeling.

## D. The chiral limit

As shown in (33), the space-like coordinate  $\psi$  can be used to describe the conserved charge associated with the conserved current  $\nu u^\rho$ . For a spacelike current, it is the conserved winding number  $N$  of a string loop such that [21]

$$N \propto \oint d\psi, \quad (51)$$

where the proportionality factor depends on the string length. For a timelike current, the same integral would yield a result similarly proportional to the conserved particle number  $Z$  present on the string. However, the physically relevant quantity is instead the invariant number

$$I^2 = N^2 - Z^2, \quad (52)$$

whose sign determines whether the current is spacelike (positive sign) or timelike (negative sign). In the gauge and reference frame chosen here, one of these parameters is set to vanish ( $Z$  for the magnetic regime and  $N$  for the electric one), while the other can be obtained by integrating the state parameter over the worldsheet.

In the magnetic regime, when quantum effects are taking place where shocks form, they lead to the emission of some part of the current, with the result of lowering the winding number  $N$ . But as in this case  $Z = 0$ , one sees that the invariant quantity  $I^2$  is lowered in the process. If the resulting loop were still unstable, it would repeat this process, and one can conjecture that the resulting stable vorton configuration will be close to chiral, for which  $N^2 = Z^2 = 0$ .

In the electric regime, the same apply with now  $N$  set originally to zero and  $Z$  decreasing as the string emits particles at each kink. Therefore, again, one find that  $|I^2|$  is lowered, up to the point where the chiral limit could be reached from the opposite end.

## VI. CONCLUSIONS

We have explored the full nonlinear evolution of superconducting cosmic string loops with rational and logarithmic equations of state [25]. Starting with elliptic configurations, i.e. far from equilibrium, and varying the state parameter in the initial conditions allowed us to examine many loop trajectories. We have also investigated the fate of unstable equatorial modes.

In the magnetic regime where the tension is constrained to be positive [9], some string loops were found to exhibit shocks, seen as discontinuities in the state parameter. Near these shocks, the longitudinal perturbation velocity may become imaginary, implying instabilities at the classical level, to be presumably understood later in terms of massive radiation, i.e., quantum instabilities leading to charge carrier emission.

For electric strings for which the constraint is  $c_L^2 > 0$ , some configurations were found to evolve to the point where the tension becomes negative, so that transverse instabilities would ultimately be transformed into, again, massive radiation.

Finally, all the configurations that were not leading to the previously described effects, i.e., those for which the classical analysis was found valid throughout their evolution, were shown to give rise to regions of very high curvature radius, a situation known to enhance considerably the escape probability for the trapped charge carrier particles.

The purely classical treatment of the evolution of current-carrying cosmic strings has therefore been proved insufficient. Further studies are now needed to find some ways of incorporating the quantum effects whose significance has been emphasized here. Once this is achieved, the evolution scheme presented here might be used in order to evaluate the rate of massive radiation during the lifetime of a characteristic loop, and its fate when back reaction is incorporated. With that knowledge, it might in turn become possible to seriously estimate the spectrum of this massive radiation. Eventually, these results should enable to derive constraints on the parameters of the problem by comparison with observed cosmological data. Note that, for the time being, it is not clear whether the effects exhibited here have a tendency to enhance or lower the vorton formation rate. On the one hand, if radiation is very efficient, it could be argued that many configurations might turn out to decay into massive radiation and currentless Goto–Nambu strings. On the other hand, if radiation is not that efficient, it could in fact accelerate the vorton formation rate by helping to form the final vorton state more quickly, and by driving this final vorton state toward the chiral limit where it is stable. The resulting distribution would then be very close to the chiral limit.

- 
- [1] T. W. B. Kibble, *J. Phys. A* **9**, 1387 (1976), *Phys. Rep.* **67**, 183 (1980).
  - [2] E. P. S. Shellard & A. Vilenkin, *Cosmic strings and other topological defects*, Cambridge University Press (1994); M. B. Hindmarsh, T. W. B. Kibble, *Rep. Prog. Phys.* **58**, 477 (1995).
  - [3] T. Goto, *Prog. Theor. Phys.* **46**, 1560 (1971); Y. Nambu, *Phys. Rev. D* **10**, 4262 (1974).
  - [4] D. Austin, E. Copeland, T. W. B. Kibble, *Phys. Rev. D* **48**, 5594 (1993); A. Albrecht, N. Turok, *Phys. Rev. Lett.* **54**, 1868 (1985); *Phys. Rev. D* **40**, 973 (1989); D. P. Bennett, F. R. Bouchet, *Phys. Rev. Lett.* **60**, 257 (1988); *Phys. Rev. Lett.* **63**, 2776 (1989); *Phys. Rev. D* **41**, 2408 (1990); B. Allen, E. P.S. Shellard, *Phys. Rev. Lett.* **64**, 119 (1990).

- [5] E. Witten, Nucl. Phys. B **249**, 557 (1985); A. C. Davis, S. C. Davis, Phys. Rev. D **55**, 1879 (1997).
- [6] A. Babul, T. Piran, D. N. Spergel, Phys. Lett. B **202**, 307 (1988).
- [7] P. Peter, Phys. Rev. D **45**, 1091 (1992).
- [8] P. Peter, Phys. Rev. D **46**, 3335 (1992).
- [9] P. Peter, Phys. Rev. D **47**, 3169 (1993).
- [10] B. Carter, in *The formation and evolution of Cosmic Strings*, ed. G. Gibbons, S. Hawking, T. Vachaspati, pp 143-178 (Cambridge U.P., 1990).
- [11] P. Peter, Phys. Lett. B **298**, 60 (1993).
- [12] B. Carter, Phys. Lett. B **404**, 246 (1997).
- [13] C. J. A. P. Martins, E. P. S. Shellard Phys. Rev. D **57**, 7155 (1998); B. Carter, P. Peter, Phys. Lett. B (1999) to appear.
- [14] B. Carter, X. Martin, Ann. of Physics **227**, 151 (1993).
- [15] X. Martin, Phys. Rev. D **50**, 7479 (1994).
- [16] R. L. Davis, E. P. S. Shellard, Phys. Rev. D **38**, 4722 (1988); Nucl. Phys. B **323**, 209 (1989); B. Carter, Ann. N.Y. Acad.Sci., **647**, 758 (1991); B. Carter, Proceedings of the XXXth Rencontres de Moriond, Villard-sur-Ollon, Switzerland, 1995, Edited by B. Guiderdoni and J. Tran Thanh Vân (Editions Frontières, Gif-sur-Yvette, 1995).
- [17] R. Brandenberger, B. Carter, A.C. Davis, M. Trodden, Phys. Rev. D **54**, 6059 (1996).
- [18] S. Bonazzola, P. Peter, Astropart. Phys. **7**, 161 (1997).
- [19] S. Yoshida et al., Astropart. Phys. **3**, 105 (1995); N. N. Efimov et al., ICRR Symposium on Astrophysical Aspects of the Most Energetic Cosmic Rays, Ed. by M. Nagano, F. Takahara, World Scientific (1991); T. A. Egorov, Proceedings of the Tokyo Workshop on Techniques for the Study of Extremely High Energy Cosmic Rays, Ed. M. Nagano, published by the Institute for Cosmic Rays Research, University of Tokyo (September 1993); J. Linsley, Phys. Rev. Lett. **10**, 146 (1963); G. Brooke et al., 19th ICRC (La Jolla) **2**, 150 (1985); A. A. Watson, ICRR Symposium on Astrophysical Aspects of the Most Energetic Cosmic Rays, Ed. by M. Nagano, F. Takahara, World Scientific (1991); M. A. Lawrence, R. J. O. Reid, A. A. Watson, J. Phys. G **17**, 733 (1991).
- [20] A. L. Larsen, M. Axenides, Class. Quantum Grav. **14**, 443 (1997).
- [21] B. Carter, P. Peter, A. Gangui, Phys. Rev. D **55**, 4647 (1997); A. Gangui, P. Peter, C. Boehm Phys. Rev. D **57**, 2580 (1998).
- [22] A. Vilenkin Phys. Rev. D **41**, 3038 (1990); B. Carter Phys. Rev. D **41**, 3869 (1990); X. Martin Phys. Rev. Lett. **74**, 3102 (1995).
- [23] B. Carter, Phys. Rev. Lett. **74**, 3098 (1995)
- [24] R. L. Davis, Phys. Rev. D **38**, 3722 (1988).
- [25] B. Carter, P. Peter, Phys. Rev. D **52**, R1744 (1995).
- [26] X. Martin, submitted to International Journals of Physics (1999).
- [27] X. Martin and P. Peter, Phys. Rev. D **51** 4092 (1995).
- [28] G. V. Vlasov, *Discontinuities on strings*, hep-th/9905040
- [29] B. Carter, Phys. Rev. Lett. **74**, 3098 (1995).
- [30] P. Peter, J. Phys. A **29**, 5125 (1996).